



OPEN

The early local and systemic Type I interferon responses to ultraviolet B light exposure are cGAS dependent

Sladjana Skopelja-Gardner¹✉, Jie An¹, Joyce Tai¹, Lena Tanaka¹, Xizhang Sun¹, Payton Hermanson¹, Rebecca Baum¹, Masaoki Kawasumi², Richard Green^{3,4}, Michael Gale Jr.^{3,4}, Andrea Kalus², Victoria P. Werth⁵ & Keith B. Elkon^{1,3,4}✉

Most systemic lupus erythematosus (SLE) patients are photosensitive and ultraviolet B light (UVB) exposure worsens cutaneous disease and precipitates systemic flares of disease. The pathogenic link between skin disease and systemic exacerbations in SLE remains elusive. In an acute model of UVB-triggered inflammation, we observed that a single UV exposure triggered a striking IFN-I signature not only in the skin, but also in the blood and kidneys. The early IFN-I signature was significantly higher in female compared to male mice. The early IFN-I response in the skin was almost entirely, and in the blood partly, dependent on the presence of cGAS, as was skin inflammatory cell infiltration. Inhibition of cGAMP hydrolysis augmented the UVB-triggered IFN-I response. UVB skin exposure leads to cGAS-activation and both local and systemic IFN-I signature and could contribute to acute flares of disease in susceptible subjects such as patients with SLE.

Sensitivity to ultraviolet B (UVB) light affects ~70% of systemic lupus erythematosus (SLE) patients and manifests as localized skin disease, cutaneous lupus erythematosus (CLE). However, acute UV exposure also instigates systemic disease flares^{1,2}. Why SLE patients have such a high frequency of photosensitivity and how sunlight exposure leads to systemic disease exacerbations in SLE remain largely unknown. The chronically elevated expression of Type-I Interferon (IFN-I) and IFN-I simulated genes (ISG or IFN signature) in peripheral blood cells³⁻⁵, lesional and non-lesional skin^{6,7}, as well as cells extracted from kidney biopsies^{7,8} provide clues to disease pathogenesis. *In vitro* studies of human keratinocytes have shown that exposure of cells to UVB light can induce an IFN-I response^{9,10}. In this study, we ask whether acute exposure to UV light *in vivo* can trigger both a local and a systemic IFN-I signature. We also address differences in the response in female and male mice, due to the overwhelming bias of SLE for females (9:1 female to male ratio)¹¹ and the recently reported sex-dependent differences in skin gene expression¹².

We have previously shown¹³ and others have recently confirmed¹⁴ that repeated irradiation with a low dose of UVB light triggered local ISG expression. In our *in vivo* study, we showed that the UVB light-triggered IFN-I response was dependent on the stimulator of interferon (IFN) genes (STING) and independent of pDC recruitment¹³. Canonically, STING has been thought to act primarily as a cytosolic DNA sensing adaptor protein downstream of cyclic GMP-AMP (cGAMP) synthase (cGAS), leading to production of IFN β and inflammatory cytokines. However, recent studies have shown that other DNA (AIM2, IFI16) as well as RNA sensors (RIG-I-MAVS) signal through or cooperate with STING to drive IFN-I production in viral immune responses^{15,16}. Involvement of the canonical cGAS-STING DNA sensing pathway in UV light-triggered IFN-I and inflammatory responses in the skin has not previously been examined.

Using a single dose of UVB light rather than repetitive stimulation (which is confounded by overlapping damage and repair responses), we first demonstrated that acute exposure to UV light triggers a strong IFN-I response

¹Division of Rheumatology, University of Washington, Seattle, WA, USA. ²Division of Dermatology, University of Washington, Seattle, WA, USA. ³Department of Immunology, University of Washington, Seattle, WA, USA. ⁴Center for Innate Immunity and Immune Disease, University of Washington, Seattle, WA, USA. ⁵Dermatology Section, Philadelphia Veterans Affairs Medical Center, Philadelphia, USA. ✉e-mail: ssg12@uw.edu; KElkon@medicine.washington.edu

in both normal mouse and human skin. Remarkably, UV light stimulated not only a local but also a systemic IFN-I response, in the blood and the kidneys. We found that the DNA sensor cGAS was important for the early local and systemic IFN signatures. Moreover, inhibiting the degradation of extracellular cGAMP by a chemical inhibitor of the cGAMP hydrolase ectonucleotide pyrophosphatase phosphodiesterase 1 (ENPP1) enhanced the magnitude of the IFN-I response to UV light.

Results

A single exposure to UVB light triggers an early cutaneous IFN-I response exaggerated in female mice. *In vitro* and *ex vivo* studies reported that UVB and UVC light-mediate cell damage induced IFN-I in keratinocytes and other cell types^{10,17}. We and others observed that repeated exposure to low doses of UVB light (100mJ/cm² per day for 5 days) caused a modest upregulation in ISG expression in the skin of normal mice^{13,14}. However, this subacute model generates cycles of inflammation and resolution, which complicates understanding as to whether IFN-I reflects immediate injury or a wound repair response. Here, we first addressed whether a single dose (500mJ/cm² in all experiments) of UVB light *in vivo* affects IFN-I production in C57BL/6J (B6) mice, a strain shown to best mirror cutaneous changes to UVB in human skin¹⁸. This, or higher doses have been widely used in the B6 mice and defined as 2 minimal inflammatory doses^{9,19}.

Gene expression analyses of skin at different times (6, 24, and 48 hours) following exposure to a single dose of UVB light demonstrated a striking increase (~10-fold) in cutaneous ISG mRNA levels: *Irf7*, *Ifit1*, *Ifit3*, *Ifi44*, *Isg15*, *Isg20*, and *Mx1*, compared to non-UV exposed baseline (Fig. 1A). The mRNA expression levels of the majority of the tested ISG remained above baseline (1.8–16 fold induction) 48 hr after exposure to UVB light, demonstrating that UVB-triggered IFN-I signaling persisted for several days (Fig. 1A). Similar to a previous report using *ex vivo* samples¹⁷, we detected a modest (~2-fold) and transient (6 hr) IFN- κ expression in the skin (not shown). Early induction in cutaneous expression of all the tested ISG was strikingly higher in female than in male mice, and the greater fold-induction of some ISG in female skin persisted at 24 hr (*Ifit3* and *Ifi44*) and 48 hr (*Ifit3* and *Irf7*) after UVB exposure (Fig. 1A). Skin IFN scores (Fig. 1B), i.e. composite scores of the relative expression of each gene at 6 and 24 hours after UVB light injury relative to the baseline levels prior to injury²⁰, were higher in female compared to age matched male mice (Fig. 1B). These data demonstrate that females exhibit a markedly exaggerated early cutaneous IFN-I response to UVB injury (as much as 10-fold compared to males at 6 hr). In light of these findings, all subsequent experiments were performed using female mice. IFN β protein production was confirmed by immunofluorescence staining of skin tissue, 6 and 24 hours after exposure to UVB light (Fig. 1C).

A single exposure to UVB light also induces an interferon signature in human skin. To test the relevance of our acute model of UV light-triggered IFN-I response in human skin, we exposed healthy volunteers (n = 5, female) to a single dose of UV light (2 MED for UVB) and performed RNA sequencing on skin biopsies from unexposed skin and skin collected 6 hr and 24 hr after UV exposure. Using a published set of IFN-I response genes⁸, we demonstrated that a single UV exposure triggered an IFN signature in healthy skin as early as 6 hr (Fig. 1D,E). Analogous to the murine studies, we observed a prominent IFN signature after UV exposure even when only the 7 genes investigated in the mouse skin were used to derive the IFN-I scores (Fig. 1F). Notably, the IFN-I scores derived from the 7 genes made up ~30% of the total IFN-score generated from the entire gene set (188 IFN-I response genes, Fig. 1E,F), suggesting that the 7 ISGs investigated in the murine studies are a reasonable representation of the overall IFN-I response in the human skin. These data for the first time demonstrate that UV light stimulates an IFN-I response in the human skin *in vivo*. Although it is well established that most SLE patients demonstrate an IFN signature in affected and unaffected skin^{7,21}, the genesis of ISGs in the skin is unknown. Our findings suggest UV light exposure as a potentially important source of IFN-I activation in the skin in humans as well as mice.

Skin exposure to UVB light triggers a systemic IFN-I response. The presence of an IFN signature in SLE patients was first detected in peripheral blood mononuclear cells (PBMC) in 2003^{3–5}. More recently, the IFN signature in PBMC was reported in patients with cutaneous lupus²² and the IFN signature in SLE skin has been linked to a similar signature in the kidneys of lupus nephritis patients^{7,8}. A key question in SLE is whether the IFN signature detected in PBMC is generated in blood or in tissues and, if in tissues, which tissues are responsible? To examine the systemic effects of UV light, we exposed mice to the single dose of UVB light and quantified ISG expression in circulating blood cells. As shown in Fig. 2A, UVB light-mediated skin injury triggered a striking upregulation in ISG mRNA levels in the peripheral blood cells (6–24 hr). Compared to the skin, where ISG expression persisted 24 hr after exposure to UVB (Fig. 1), the kinetics of ISG expression in the blood varied. Expression levels of most genes peaked early, while others were higher at 24 hr (*Isg15* and *Isg20*) after UVB injury (Fig. 2A), possibly reflecting a second wave of injury, infiltration of immune cells, different DAMPs, or other mechanisms. The cumulative IFN scores reflect rapid induction in IFN signature in blood cells following skin exposure to UV light (Fig. 2B). Similar to the findings in the skin, female mice demonstrated a heightened early IFN-I response in circulating blood cells after exposure to UVB light (Supplementary Figure S1). The early IFN response in the blood was accompanied by increased IFN β concentration in the plasma 6 hr after exposure to UVB light (Fig. 2C). Of relevance to human SLE, pre-treatment of mice with hydroxychloroquine (HCQ), a TLR and cGAS antagonist²³ that has demonstrated efficacy in treating cutaneous lupus in patients with an IFN signature²⁴, significantly decreased the early IFN-I scores in both the skin and the blood after exposure to UVB light (Fig. 2D).

Since recent studies reported that presence of an IFN signature in keratinocytes associates with lupus nephritis, as well as with an IFN signature in kidneys^{7,8}, we asked whether UV light exposure of the skin could impact ISG expression in the kidneys. Indeed, 24 hr after skin exposure to UVB light, we observed an increase in ISG expression levels in kidneys (Fig. 2E), which could not be attributed to circulating blood cells as the kidneys had

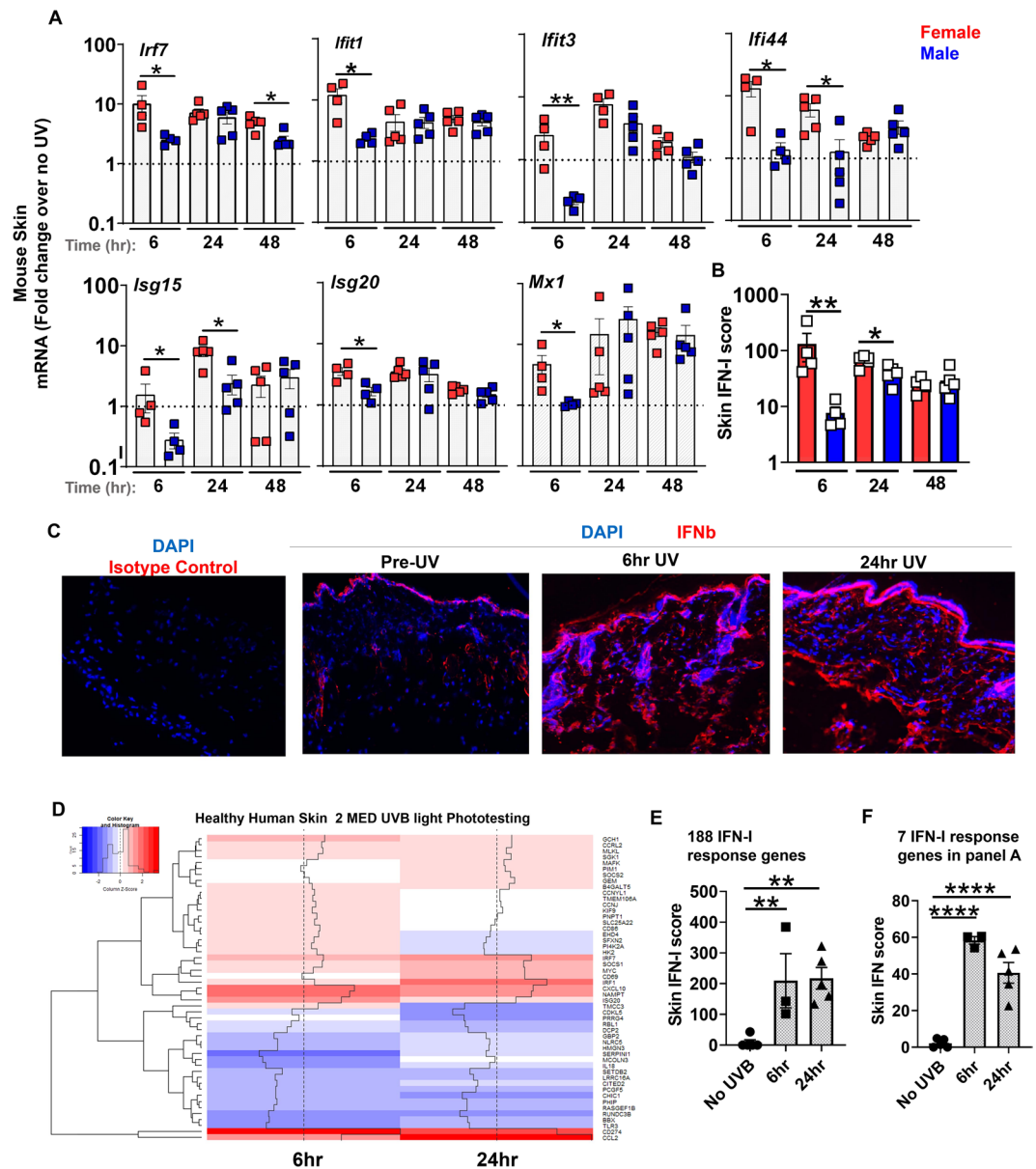


Figure 1. A single exposure of skin to UVB light triggers an early ~10-fold induction of type I IFN-stimulated genes (ISG) in female mice and induces interferon gene expression in human skin. Age-matched male and female B6 mice were shaved dorsally and the whole back was exposed to one dose of UVB light (500 mJ/cm²). At 6, 24, and 48 hours after UV irradiation, (A) fold induction in the expression of type I IFN stimulated genes (ISG) in the skin: *Irf7*, *Ifit1*, *Ifit3*, *Ifi44*, *Isg15*, *Isg20*, and *Mx1* was determined relative to baseline, i.e. non-irradiated skin (no UV). (B) Skin IFN scores for female and male B6 mice at 6, 24, and 48 hr after UVB light irradiation were calculated as sum of normalized expression levels of the same 7 ISG as discussed in Methods. (C) Immunofluorescence staining of IFNβ (red) in mouse skin tissues prior to, 6 hr, and 24 hr after UV exposure. Rabbit IgG isotype control staining in the left-most panel. Nuclear staining in DAPI. (D–F) IFN-I response was evaluated in healthy human volunteers 6 and 24 hr after UV exposure (2 MED UVB) and the ISG most differentially expressed shown in the heatmap (D). IFN scores were derived based on (E) 188 published IFN-I response genes⁸ or (F) 7 ISGs used in mouse studies (B). Statistical significance was determined by (A,B) Student's t-test (n = 4–5; *p < 0.05, **p < 0.01) or (E,F) one-way ANOVA (n = 3–5; **p < 0.01, ***p < 0.0001).

been perfused prior to harvest. The increase in Sca1 on intra-renal B cells (Fig. 2F) confirmed IFN-I exposure of cells²⁵ in the kidney. Whether the IFN signature is produced by the direct influence of IFNβ, release of DAMPs from the skin, or even tissue infiltration by IFNβ producing cells that have migrated from the blood after skin exposure to UVB remain to be determined. Since ISG expression in the kidney did not show the same striking changes as were observed in skin 6 hr after exposure to UV light (Supplementary Figure S2), the delayed IFN-I response in the kidney may well reflect release of DAMPs or infiltration by immune cells. In summary, analysis of blood and kidneys revealed that UV exposure of skin can act as a source of the systemic IFN-I in SLE, including the kidney.

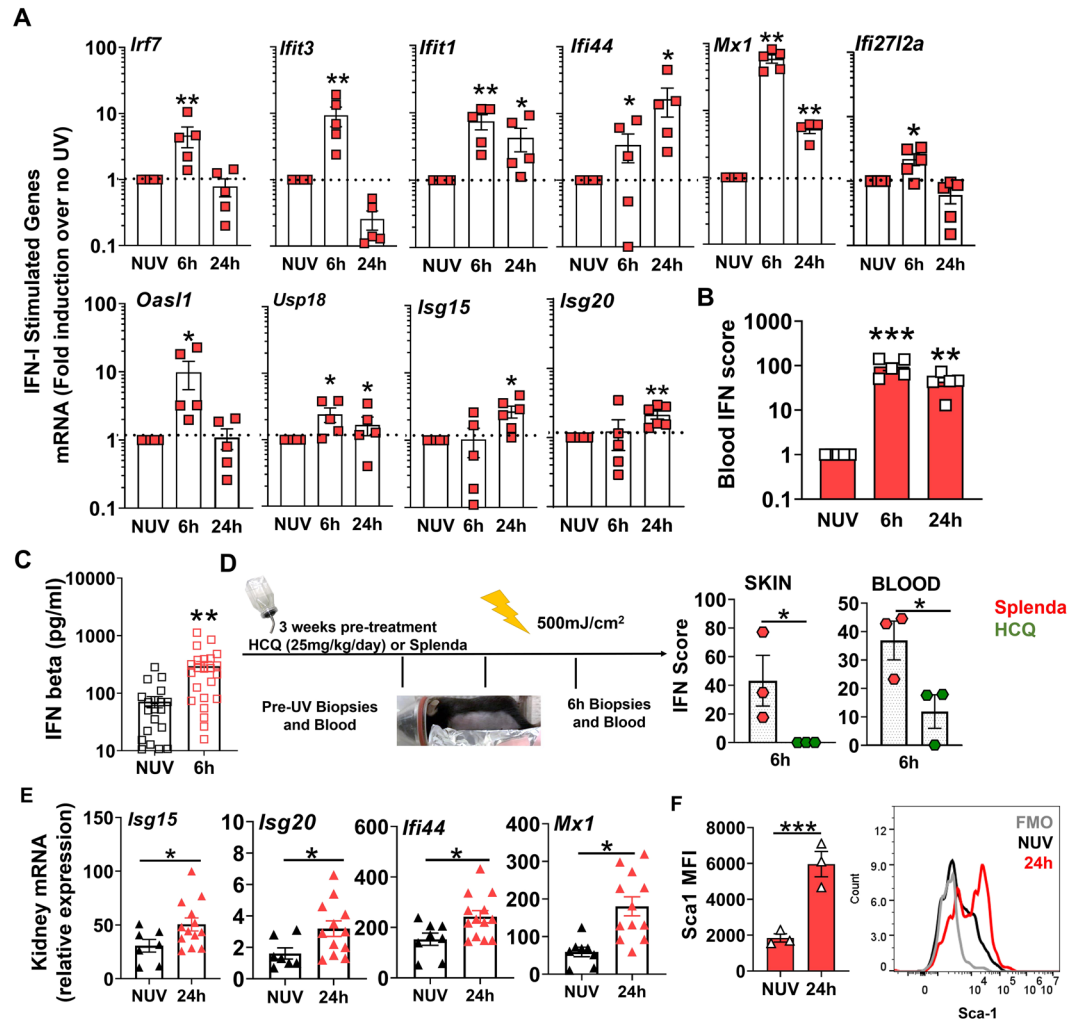


Figure 2. Acute skin exposure to UVB light triggers a systemic IFN-I response. Female B6 mice were exposed to a single dose of UVB light as in Fig. 1, except that only half of the back was exposed. **(A)** Fold induction in ISG mRNA levels in the peripheral blood cells 6 and 24 hr after skin exposure to UVB light was determined relative to mRNA levels in the blood prior to UV. **(B)** Blood IFN scores were calculated as the sum of normalized expression levels of the 7 most highly expressed ISGs after UV exposure (*Mx1*, *Ifit1*, *Ifit3*, *Ifi44*, *Usp18*, *Oas1*, and *Ifi2712a*). **(C)** IFN β concentration in plasma prior to UV (No UV, NUV) and 6 h after UV light exposure in B6 mice. **(D)** B6 mice were treated with hydroxychloroquine (HCQ, 25 mg/kg/day) or Splenda (controls) for 3 weeks prior to UV irradiation. Blood and skin IFN scores for both treatment groups were determined for samples 6 hr after UV exposure. **(E)** Relative expression of representative ISG transcripts in the perfused kidney tissues of B6 mice at baseline (no UV, NUV) or 24 h after skin exposure to UVB light. **(F)** Flow cytometry analysis of Sca-1 expression, presented as mean fluorescence intensity (MFI), on B cells in perfused kidney tissue prior to (NUV) and 24 h after UV exposure. Statistical significance was determined by Student's t-test ($n = 4-5$ A,B; $n = 23$, C; $n = 3$, D; $n = 7-12$, E; $n = 3$, F; * $p < 0.05$, ** $p < 0.01$, *** $p < 0.001$).

cGAS is essential for the early cutaneous IFN-I response to UVB light. UV light is genotoxic, cytotoxic, and generates modified nucleic acids such as oxidized DNA¹⁰. Recently, in a repetitive UV exposure model, we observed that IFN-I and inflammatory cytokines induced by UVB light were markedly reduced in STING deficient mice¹³. Canonically, STING has been thought to act primarily as a cytosolic DNA sensing adaptor protein downstream of cGAS. Upon engaging the cGAS synthesis product 2'3' cGAMP, STING undergoes a conformational change to bind TANK binding kinase 1 (TBK1) and enables the phosphorylation of interferon regulatory factor 3 (IRF3) as well as activation of IKK β and NF κ B, leading to production of IFN-I and inflammatory cytokines, respectively¹⁵. However, other DNA (AIM2, IFI16, DAI) as well as RNA sensors (RIG-I-MAVS) can signal through, or cooperate with, STING so as to drive IFN-I production following certain viral infections^{15,16}. Whether skin inflammation provoked by UV light triggers DNA to activate the canonical cGAS-STING pathway *in vivo* is not known. We therefore compared the ISG mRNA expression levels 6 and 24 hours following a single UVB light exposure of age-matched female B6 (wild type, WT) or *cGAS*^{-/-} B6 mice, which have previously been shown to have intact TLR and other sensor pathways²⁶. Whereas no difference in baseline (no UVB) skin ISG mRNA levels was found between WT and *cGAS*^{-/-} mice (not shown), we observed that *cGAS* deficiency

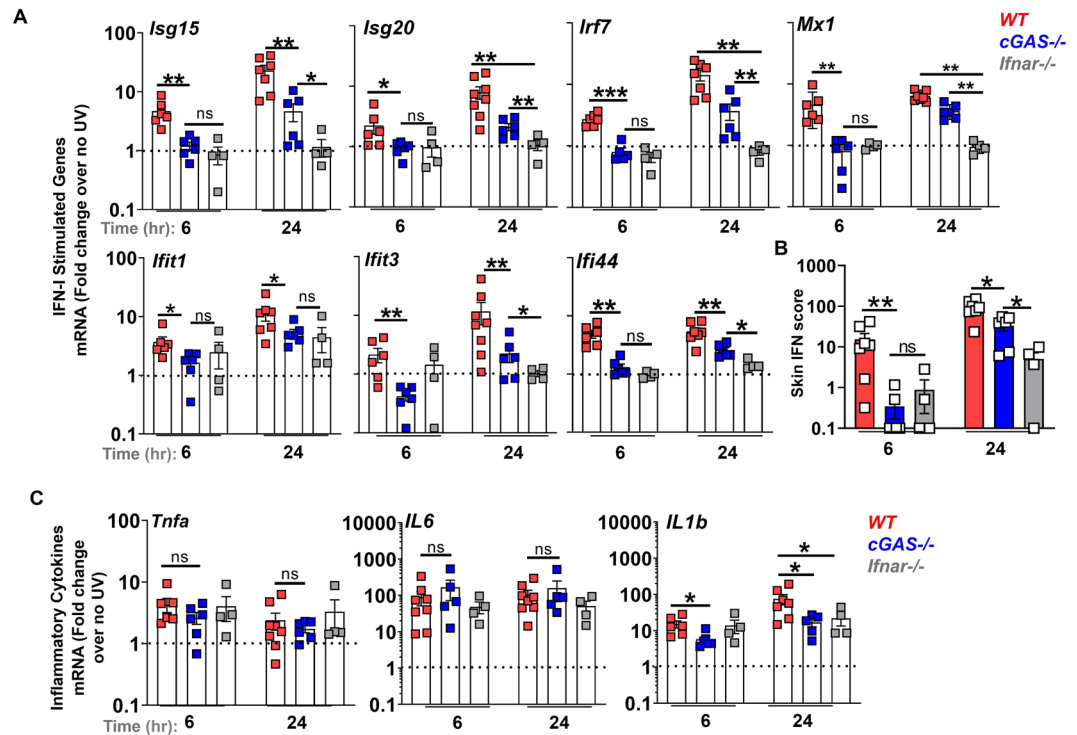


Figure 3. The early skin IFN response to UV light exposure is cGAS dependent. Age-matched female B6 (wild type, WT), *cGAS*^{-/-}, and *Ifnar1*^{-/-} mice were exposed to a single dose of UVB light as in Fig. 2. Skin biopsies were obtained prior to UVB light exposure and at 6 and 24 h after irradiation. **(A)** Fold change in the expression of IFN-I stimulated genes (ISG) in the skin was determined relative to baseline, i.e. non-irradiated skin (no UV). **(B)** Skin IFN scores at 6 and 24 hours after UVB were calculated as sum of normalized expression levels of the same 7 ISG. **(C)** Fold-induction in the expression of inflammatory cytokines *Tnfa*, *Il-6*, and *Il1-β* were determined relative to baseline, i.e. non-irradiated skin (no UV). Statistical significance was determined by Student's t-test (n = 4–8; *p < 0.05, **p < 0.01, ***p < 0.001, ns = not significant).

almost completely abrogated the early (6 hr) cutaneous ISG expression after exposure to UVB (Fig. 3A). The lack of early ISG induction in *cGAS*^{-/-} mice was comparable to that of IFN- α/β receptor deficient controls (*Ifnar*^{-/-}) (Fig. 3A). While ISG expression in the *cGAS*^{-/-} skin was detected 24 hr after exposure to UVB, the fold-increase in ISG levels was substantially lower compared to WT controls (45.7% (*Ifit1*)– 84.1% (*Ifit3*) reduction) (Fig. 3A). However, ISG mRNA levels in *cGAS*^{-/-} skin were significantly higher than in *Ifnar*^{-/-} controls at this later time point (Fig. 3A). Cumulative skin IFN scores confirmed that cGAS was required for the early cutaneous IFN signature after UVB injury, as ISG expression was not increased in *cGAS*^{-/-} mice at 6 hr. While later IFN-I scores in *cGAS*-deficient mice were lower than those in WT skin, they were significantly higher than in the *Ifnar*^{-/-} controls (Fig. 3B), indicating that cGAS-independent pathways contributed to the IFN signature in the skin exposed to UV light over time. At this later time point, a modest increase in some ISGs (*Ifit1*, *ifi44*, Fig. 3A) in *Ifnar*^{-/-} mice is consistent with previous reports of IFN-independent activation of these particular genes through IRF3-mediated gene expression^{27,28}. Together, these data confirm that the requirement for cGAS in the cutaneous IFN-I response to UVB is temporally regulated. The same temporal requirement for cGAS was observed in male mice, despite the more modest increase in the early ISG expression (Supplementary Figure S3). cGAS is essential for the early (6 hr) activation of IFN-I signaling and the cGAS-STING pathway is the dominant but not sole contributor to IFN-I activation in the skin later (24 hr) following exposure to UVB.

TNF and IL-6 gene expression are stimulated via a cGAS-independent pathway following skin exposure to UV light. Since the cGAS-STING pathway has been implicated in the regulation of inflammatory cytokines through NF κ B-mediated transcriptional activation of TNF and IL-6 or by activation of the inflammasome and generation of IL-1 β ²⁹, we next asked whether UVB-triggered cGAS activation is necessary to induce these cytokines. We found that a single high dose of UVB light induced rapid expression (6 hr) of TNF, IL-6, and IL-1 β but that the extent of the TNF and IL-6 response was equivalent in WT and *cGAS*^{-/-} mice (Fig. 3C). In contrast to TNF and IL-6, IL-1 β mRNA levels were significantly lower in *cGAS*^{-/-} skin both 6 and 24 hr after UVB exposure (Fig. 3C). A significant reduction in IL-1 β gene expression was also detected in IFNAR deficient mice (Fig. 3C). Together, our findings demonstrate that the DNA sensing cGAS-STING pathway is important for the generation of IFN-I and IL-1 β , but not for stimulation of TNF and IL-6 gene expression following skin exposure to UV light.

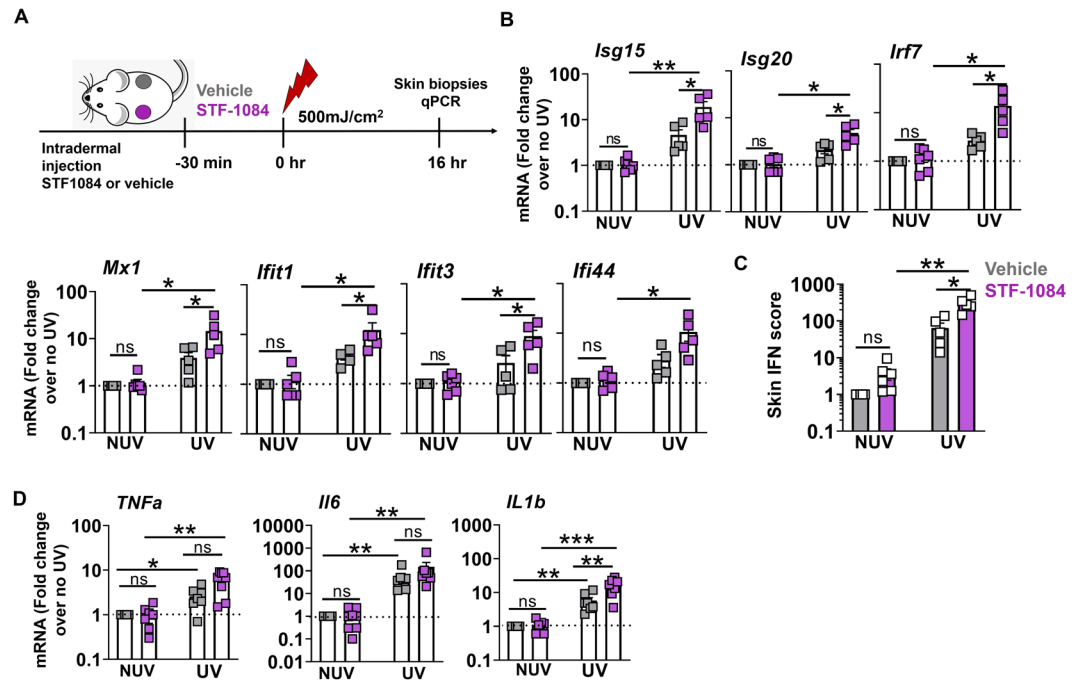


Figure 4. Extracellular cGAMP exaggerates the IFN-I, but not the IL-6 or TNF, response to UVB light. (A) B6 mice were shaved and injected intradermally with 100 μ M ENPP1 inhibitor (STF-1084) or Vehicle (PBS), 30 min prior to the exposure to UVB light as above. Skin was biopsied 16 hr after UV exposure. (B) Fold-change in ISG expression was determined relative to vehicle-treated non-UVB exposed skin in three treatment groups: STF1084 without UVB, vehicle with UVB, and STF-1084 with UVB. (C) Skin IFN scores in vehicle and STF-1084-treated UV exposed and non-exposed (NUV) skin were calculated as sum of normalized expression levels of the same 7 ISG as in Fig. 1. (D) Fold-induction in the expression of inflammatory cytokines *Tnf α* , *Il-6*, and *Il-1 β* were determined relative to baseline, i.e. non-irradiated vehicle-treated skin (no UV). Statistical significance was determined by Student's t-test ($n = 5$, 2 independent experiments; * $p < 0.05$, ** $p < 0.01$, ns = not significant).

Extracellular cGAMP contributes to the cutaneous IFN-I and IL-1 β response to UV light. Since extracellular export of the cGAS product, cGAMP, plays a role in the induction of IFN-I following radiation therapy³⁰, we asked whether release of cGAMP following UVB radiation injury impacts IFN-I stimulation in the skin. To address this question, we inhibited the cell surface membrane enzyme ectonucleotide pyrophosphatase phosphodiesterase 1 (ENPP1), which hydrolyzes cGAMP^{30,31}, shortly before skin exposure to UVB (Fig. 4A). The ENPP1 inhibitor, STF-1084³⁰, led to a significantly greater induction in individual ISG expression as well as the cumulative IFN scores, compared to both the vehicle-treated skin exposed to UVB, as well as to the unexposed skin treated with the ENPP1 inhibitor (Fig. 4B,C). Consistent with findings that cGAS was not required for UVB light-triggered TNF and IL6 production (Fig. 3C), inhibition of ENPP1 did not exaggerate cutaneous TNF and IL6 mRNA expression in response to UVB light injury (Fig. 4D). However, inhibition of cGAMP hydrolysis enhanced IL-1 β mRNA levels in the skin after UV exposure (Fig. 4D), confirming that DNA sensing by cGAS contributes to IL-1 β expression in UVB light-exposed skin (Fig. 3C). These data suggest that UVB exposure triggers cGAMP release which, in turn, amplifies the IFN signature and IL-1 β , but not TNF and IL6, response.

cGAS mediates the systemic IFN-I response to UV exposure of the skin. Similar to the findings in the skin, early ISG expression in peripheral blood was largely abrogated in cGAS (by 45.1% (*Ifit1*) – 95% (*Ifi44*) decrease) as well as IFNAR (~93% decrease) -deficient mice although the extent to which specific ISGs were affected differed (Fig. 5A). At 24 hr after UVB injury, the expression levels of the majority of ISGs upregulated in WT mice were lower in the blood of cGAS $-/-$ animals (by 57% (*Mx1*)–88% (*Usp18*), Fig. 5A). To average the differences in the UV light-stimulated IFN signature in the 3 genotypes, we calculated the blood IFN scores using expression levels of 7 most-highly expressed ISGs. Overall, cGAS deficient mice demonstrated significantly lower blood IFN-I scores than their cGAS-sufficient counterparts, at both 6 and 24 hr after UV light exposure (Fig. 5B). However, peripheral blood cell IFN-I scores in cGAS $-/-$ mice were higher than in the *Ifnar* $-/-$ controls 24 hr post exposure indicating that other sensors besides cGAS also played a role at this time (Fig. 5B). Consistent with the lack of the IFN signature early in the blood of cGAS $-/-$ mice (Fig. 3B), we could not detect a significant increase in the levels of circulating IFN β (Fig. 5C) or upregulation of Sca-1 expression on cGAS deficient B cells (Fig. 5D). Therefore, in addition to the cutaneous response, cGAS is an important contributor to the early IFN-I response in the blood following a single exposure to UVB light.

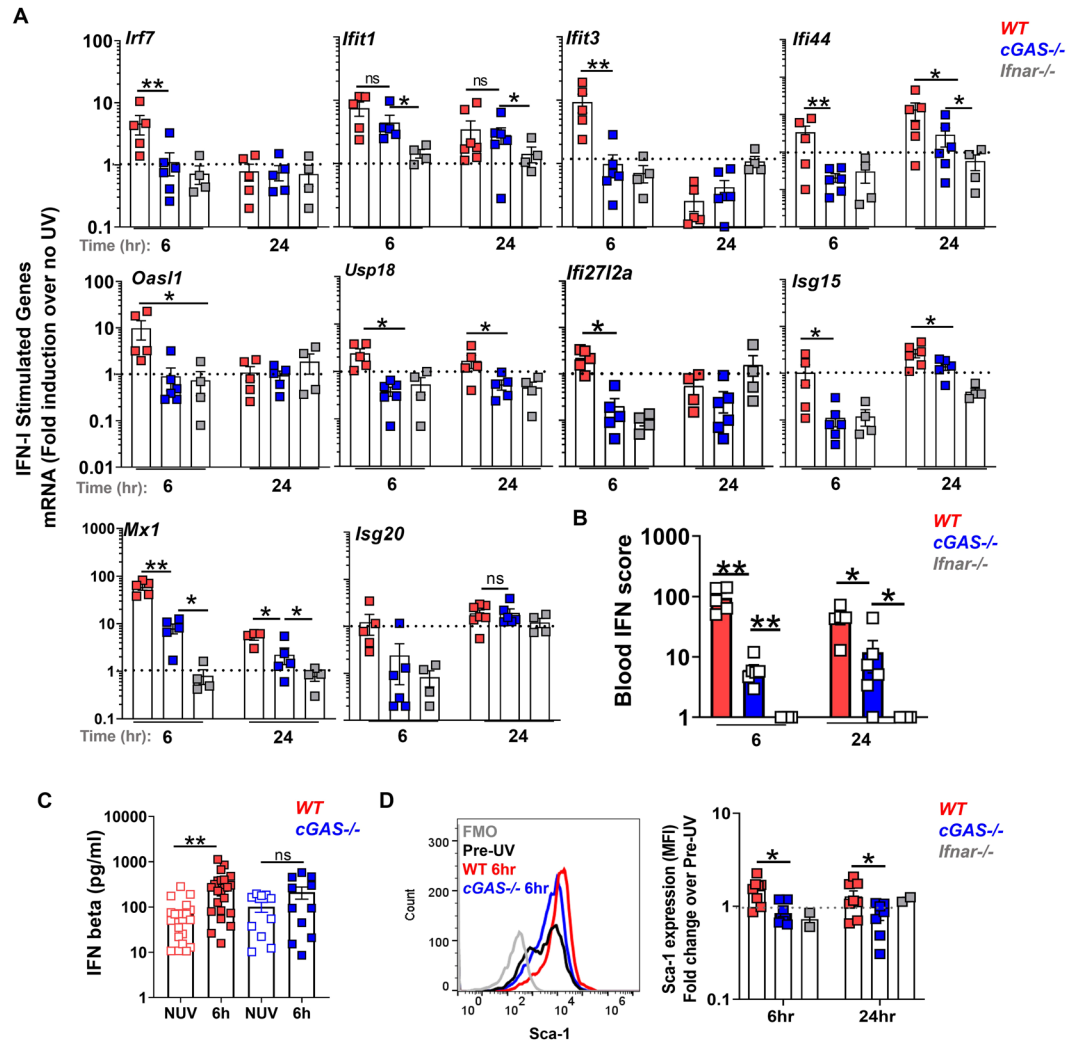


Figure 5. cGAS contributes to the systemic IFN-I response to skin UV light exposure. Age-matched female B6 (wild type, WT), *cGAS*^{-/-}, and *Ifnar1*^{-/-} mice were exposed to a single dose of UVB light as in Fig. 2. (A) Fold induction in ISG mRNA levels in the peripheral blood cells 6 and 24 hr after skin exposure to UVB light was determined relative to mRNA levels in the blood prior to UV. (B) Blood IFN scores for each genotype were calculated as the sum of normalized expression levels of the 7 most highly expressed ISGs after UV exposure (*Mx1*, *Ifit1*, *Ifit3*, *Ifi44*, *Usp18*, *Oasl1*, and *Ifi2712a*). (C) IFN β concentration in plasma prior to UV (No UV, NUV) and 6 h after UV light exposure in wild-type (WT) and *cGAS*^{-/-} mice. (D) Flow cytometry analysis of Sca-1 expression on B cells in the blood of wild type (WT), *cGAS*^{-/-}, and *Ifnar*^{-/-} mice 6 and 24 hr after UVB exposure, presented as fold change relative to non-irradiated skin cells. Representative histograms are shown for B cell population. Statistical significance was determined by Student's t-test (n = 4–6, A,B; n = 11–23, C; n = 3–8, D; *p < 0.05, **p < 0.01, ns = not significant).

Absence of cGAS dampens the innate cellular inflammatory response in UV light-exposed skin.

Analogous to inflammation triggered by infection³² and our observations of UVB light mediated sterile inflammation in the subacute model¹³, the acute response to UVB light in the skin was characterized by infiltration of neutrophils (CD11b + Ly6C^{int}Ly6G^{hi}) as well as inflammatory monocytes (CD11b + Ly6C^{high} Ly6G^{neg}) at the site of injury (Fig. 6A,B). Besides innate myeloid immune cells, exposure to UVB triggered an increase in the number of $\gamma\delta$ + (Fig. 6C) T cells in the skin of WT mice. The number of both myeloid as well as $\gamma\delta$ + T cell populations early (6 hr) after UVB exposure was significantly reduced in the skin of *cGAS*^{-/-} mice (Fig. 6A,D). The diminished skin infiltration of inflammatory monocytes in *cGAS*^{-/-} mice was sustained 24 hr after UVB exposure (Fig. 6B). Therefore, in addition to driving both the local and the systemic acute IFN-I response, cGAS-mediated DNA sensing regulates the magnitude of the cellular infiltration into UV light-injured skin. IFNAR deficient mice also had a reduced infiltration of immune cells into the skin compared to WT mice (Supplementary Figure S4), indicating that IFN-I contributes to cellular inflammation triggered by acute (i.e. a single dose) exposure to UVB light.

To investigate whether diminished immune cell infiltration in the absence of cGAS was due to muted chemotactic responses following skin exposure to UV light, we evaluated the expression of different chemoattractants.

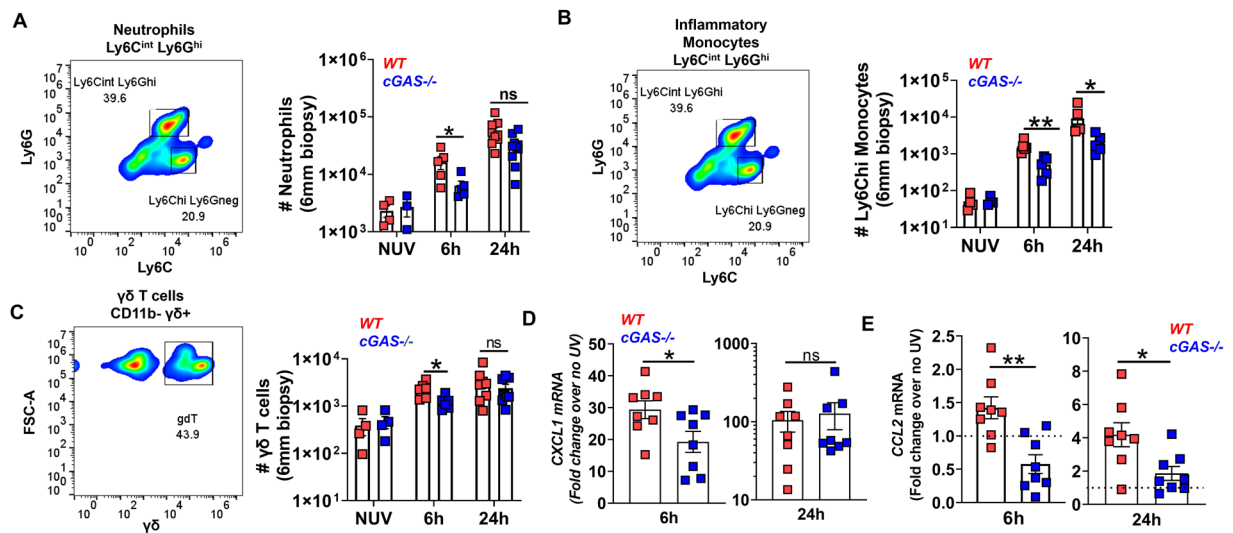


Figure 6. The innate inflammatory response to UVB light in the skin is diminished in the absence of cGAS. Age-matched female B6 (wild type, WT) and *cGAS*^{-/-} mice were exposed to a single dose of UVB light as in Figs. 2,3. Flow cytometry analysis of skin was performed and the number of (A) neutrophils (CD45 + CD11b + Ly6C^{int}Ly6G^{hi}), (B) inflammatory monocytes (CD45 + CD11b + Ly6C^{hi}Ly6G^{neg}), and (C) $\gamma\delta$ + T cells (CD45 + CD11b- $\gamma\delta$ +) were determined based on total cell number per skin biopsy (6mm). Skin biopsies from 2–4 mice were pooled for the 6h time point. (D–E) Gene expression levels of CXCL1 (D) and CCL2 (E) in the skin were quantified by QPCR. Statistical significance was determined by Student's t-test (n = 4–8; *p < 0.05, **p < 0.01, ns = not significant).

Besides diminished production of IL-1 β (Fig. 3C), we found reduced early expression of CXCL1 (Fig. 6D), both of which could contribute to lower neutrophil recruitment in the absence of cGAS. Lower cutaneous CCL2 expression in *cGAS*^{-/-} mice (Fig. 6E) could explain the reduced monocyte as well as $\gamma\delta$ + T cell^{33,34} numbers in skin. Together, our data indicate that DNA sensing by cGAS contributes to innate immune cell recruitment to UVB light exposed skin, possibly directly through IFN-I signaling and secondarily involving inflammasome activation and chemokine regulation.

Discussion

In this *in vivo* study of the inflammatory effects of UVB light exposure, we report a number of novel observations. A single exposure to UVB light is sufficient to stimulate a robust IFN-I response in both murine and human skin. In mice, the early (6 hr) IFN-I response is strikingly increased in females and the response is entirely cGAS dependent. Remarkably, not only does UVB exposure induce a local IFN signature, it also stimulates a systemic IFN-I response as determined by IFN signatures in the blood and kidney. The early blood IFN-I response was dependent on cGAS and was inhibited by hydroxychloroquine, which is consistent with our findings that aminoquinoline antimalarial drugs inhibit DNA activation of cGAS *in vitro* and *in vivo*^{23,35}. Finally, we demonstrate that cGAS also impacts the cellular inflammatory response to UV light, as evidenced by reduced numbers of innate immune cells in the UV light-exposed skin of cGAS deficient mice.

The detection of an IFN signature in the blood of SLE patients was a landmark discovery^{3–5}, but where and how IFN-I is generated is not known. Here, we show that a single exposure of skin to UV light can generate an IFN signature in both the blood and kidneys of normal mice. Since ~70–85% of SLE patients are photosensitive and the skin has a vast surface area, it is plausible that IFN-I generated in the skin and released into the circulation is, at least in part, responsible for the blood IFN signature in SLE patients. That skin might be a source of systemic IFN-I in SLE is further supported by recent findings showing a 480-fold greater ISG expression in SLE non-lesional skin versus only a 7.8-fold in the SLE blood, relative to healthy controls³⁶. Intriguingly, individuals at-risk for developing SLE (ANA +, treatment naïve, ≤ 1 clinical criteria) also have a significant skin (28.7-fold increase) but lower blood IFN signature (2.2 fold increase) compared to healthy individuals³⁶.

The significance of blood cell exposure to IFN-I following irradiation of skin with UVB is the potential for immune activation, especially in a genetically susceptible host. IFN-I can activate almost all cells in the immune system^{37,38} and Blanco *et al.*³⁹ showed that IFN-I in SLE blood causes differentiation of monocytes to DC with potent antigen presentation properties. Since many, but not all, clinical studies reveal an association between disease activity and the magnitude of the blood IFN-score^{40,41}, the generation of an IFN signature in blood following UV exposure may well explain disease exacerbations associated with sunlight exposure^{1,42}. Apart from diffusion of IFN β , release of DAMPs, cell trafficking, or some combination of these factors may contribute to the blood IFN signature following exposure of skin to UVB.

In patients with cutaneous lupus, pDC are observed in lesional skin²¹. Furthermore, a Phase I/II clinical trial suggests that pDC depletion /inhibition (anti-BDCA2 therapy) ameliorates skin disease in cutaneous lupus patients⁴³. Consistent with activation of the cGAS-STING pathway and failure to detect plasmacytoid dendritic

cells (pDC) in the skin in our previous short-term UV study¹³, we observed that skin exposure to UVB light triggered an early local and systemic increase in IFN β whereas pDC were present at low levels relative to a tape strip model (Supplementary Figure S5). These findings could be explained by the fact that we are examining acute responses in healthy mouse skin versus immunopathological observations in lupus patients with chronic disease, circulating autoantibodies, and a variety of other immunologic abnormalities. Whereas exposure of pDC to ribonucleoprotein (RNP) containing immune complexes activates TLR7 resulting in high concentrations of IFN α *in vitro*⁴⁴, it should be noted that pDC also produce IFN β following cGAS-STING activation⁴⁵. Besides pDC, keratinocytes have been proposed to be an important source of type I interferons, specifically IFN- κ and IFN β ⁴⁶. Sarkar *et al.* have reported an elevated baseline IFN- κ production by SLE keratinocytes and demonstrated that IFN- κ contributes to and amplifies the IFN signature found in SLE skin¹⁷. While the ability of keratinocytes to make IFN β has been long recognized and recently confirmed^{36,47}, analysis of the IFN signature in the skin of SLE patients strongly suggested a predominantly IFN β driven gene response⁴⁸. In this analysis, the IFN β signature was associated with increased presence of and ISG expression in monocytes, suggesting this cell type was either a major contributor or responder to the IFN β production in SLE. More detailed studies of the cell source as well as evolution of the IFN response following UVB exposure in normal and autoimmune prone strains will be needed to fully evaluate the role of different IFN-I species over time.

The recently discovered cytosolic DNA sensing cGAS-STING pathway has been implicated in generating IFN-I in response to viral infections⁴⁹, autoinflammatory and autoimmune disorders^{50–52}, tumor cell-derived DNA, as well as DNA damage triggered by chemo- or radiation therapy in tumors^{53,54}. Here, we observed that both local and systemic early production of IFN-I following skin exposure to UV light was almost entirely cGAS dependent. However, cGAS was not the sole contributor to the IFN-I response one day after UV exposure, demonstrating a temporal regulation of the mechanisms driving the IFN signature in response to UV light. Similar temporally distinct roles for different DNA and RNA sensors have been described in virus infections. For example, following HSV1 infection, both cGAS and IFI16 were required for the early (6 hr) IFN β or TNF response but RIG-I was necessary for cytokine production at a later time point (16 hr)⁵⁵. In a different study, a novel nucleic acid sensor LSm14A was found to be crucial for the early (6–9 hr) IFN β response to DNA and RNA viruses, prior to RIG-I and STING-mediated IFN-I activation, respectively⁵⁶. Numerous nucleic acid sensors have been implicated in generating the type I interferon in SLE pathogenesis⁵⁷. In the absence of cGAS, cytosolic DNA could potentially be sensed by AIM2, IFI16, or DEAD-box helicase (DDX) DNA sensors. Alternatively, if cytoplasmic RNA is the trigger of IFN-I signaling, retinoic acid inducible gene I (RIG-I), melanoma differentiation-associated gene 5 (MDA5), or RNA-activated protein kinase (PKR) could contribute to IFN-I production in mice. Endosomal TLR sensing of both DNA and RNA provides additional pathways for IFN-I activation. The temporal regulation seen in our studies could be explained by two stages of DNA injury and cell death: initially, cGAS-STING provides a rapid response to DNA damage (possibly oxidized DNA⁴⁰), while the infiltrating immune cells that die independently of UV exposure subsequently engage other nucleic acid sensors. Future studies will address whether other DNA and/or RNA sensing pathways that signal through or independently of STING contribute to the sustained IFN-I response after exposure to UV light.

UV irradiation triggers a number of biologic pathways in the skin including DNA damage, DNA repair, cell death, inflammation and resolution of skin damage^{58,59}. Pathways of DNA damage and repair are complex and have been examined in response to UV light and ionizing radiation in the skin^{60,61}. The inflammatory cytokine response in mouse skin includes increased expression of TNF, IL-6, and IL-1 β ^{9,60}. Interestingly, we found that cGAS was required for stimulation of IFN-I response, but not TNF or IL-6 mRNA expression, in response to UV light. This selectivity suggests that the cGAS-STING pathway predominantly activates IRF-3 in UV light injured skin, while other pathways provide the main source of NF- κ B signaling in this context. Two pathways stand out as possible contributors to this early inflammatory cytokine response as well as the later IFN-I response: TLR-3, which was responsible for stimulating TNF expression in response to UV light-triggered RNA damage⁹, and ATM-IFI16-STING, which predominantly activated NF- κ B and IL-6 production in response to etoposide-mediated DNA damage¹⁵. In addition to regulating the IFN-I response to UV light, we demonstrated that cGAS contributed to IL-1 β expression in UV light exposed skin. While the relationship between IFN-I and IL-1 β is complex, studies have shown that cGAMP can prime and activate the NLRP3 inflammasome^{29,62} likely explaining why IL-1 β is lower in cGAS deficient compared to WT mice following exposure to UV light. A caveat in our studies is that only mRNA, but not protein, levels were measured. Future studies will address the effect of cGAS deficiency on inflammatory protein release following exposure to UVB light.

cGAMP is the cyclic dinucleotide messenger that engages STING to trigger transcription of IFN-I⁴⁹. Recent studies of the cGAS-STING pathway in anti-tumor immunity have demonstrated that cGAMP can be released into the extracellular space where its lifespan is regulated by ENPP1, a cell surface phosphodiesterase that hydrolyzes cGAMP to AMP and GMP³⁰. Interestingly, our findings that chemical inhibition of ENPP1 exaggerated the IFN-I response to UV light suggest that hydrolysis of extracellular cGAMP is an important regulatory mechanism following UV light stimulated inflammation. The disruption in cGAMP regulation also led to enhanced IL-1 β , but not TNF or IL6, gene expression, reinforcing the selectivity for the cGAS-STING-IRF3 pathway in shaping the inflammatory response to UV light. Whether a dysregulation in ENPP1 mediated hydrolysis of extracellular cGAMP could contribute to enhanced and persistent IFN signature in SLE skin, particularly in non-lesional areas, warrants investigation.

The ability of the cGAS-STING pathway to shape the inflammatory response via IFN-I signaling was recently identified in both spontaneous and radiation therapy-induced anti-tumor immunity^{63,64}. Here, we found reduced infiltration of innate immune cells in the UV light exposed skin in the absence of cGAS. In the anti-tumor response, cGAS-STING activation was required for the recruitment of tumor specific CD8 + T cells and their infiltration into the tumor environment^{65–67}. These effects were largely attributed to the IFN-I response gene CXCL10, a recognized CD8 + T cell chemoattractant^{63,68,69}. The role of cGAS in innate immune cell recruitment

is less well established. Decreased neutrophil and inflammatory monocyte infiltration in UV light injured skin in cGAS deficient mice suggests an important role for the cGAS-STING pathway in shaping the innate immune inflammatory response. Diminished expression of neutrophil chemoattractants IL-1 β and CXCL1 as well as monocyte chemokine CCL2 in the absence of cGAS provide a model by which DNA sensing influences innate chemotactic responses in UV light injured skin. While the effect of cGAS-STING signaling on monocyte recruitment in other inflammatory contexts is yet to be illuminated, cGAS-STING pathway appears to differentially influence neutrophil recruitment in infectious vs. sterile tissue injury^{70,71}. The significantly reduced recruitment of both neutrophils and inflammatory monocytes in the absence of IFNAR suggests an important role for IFN-I production in regulating myeloid cell recruitment to the skin in response to acute exposure to UV light, in contrast to what was observed with the low dose repetitive UV exposure reported previously¹³. While our understanding of the role played by $\gamma\delta$ + T cells in UV-light exposed skin is limited, MacLeod *et al.* have previously proposed that skin resident $\gamma\delta$ + T cells contribute to DNA repair following exposure to UV light⁷² and our data suggest that cGAS-mediated DNA sensing contributes to $\gamma\delta$ + T cell recruitment in response to UV light. These results, together with the report of $\gamma\delta$ + T cells in the skin of chronic CLE patients⁷³ and findings that $\gamma\delta$ + T cells contributed to the cellular inflammatory response and skin pathology in TLR-7 mediated CLE murine model⁷⁴, call for further examination of $\gamma\delta$ + T cells in SLE.

Besides providing novel mechanistic insights into the inflammatory response to UV light, our studies also introduced an important sex-dependent distinction in this response. The early skin IFN-I response to UV light was almost 10-fold higher in females compared to males which is of considerable interest considering the 9:1 female to male prevalence of SLE¹¹. Whether this response can be explained by differential upregulation of the transcription factor, VGLL3, which is associated with heightened baseline expression of immune genes in the female skin¹² remains to be determined. Interestingly, the greater ISG response in the skin in females is not restricted to provocation by UV light as females had higher ISG expression in response to HIV infection, possibly contributing to a greater protective role at the epithelial and mucosal surfaces⁷⁵.

In summary, our findings indicate that exposure to UV light provokes a local and systemic IFN signature. IFN-I is stimulated initially via cGAS activation and this acute activation could mechanistically link UV light to flares of disease in SLE. In normal situations, acute inflammation is resolved through many reparative mechanisms that involve T-regulatory cells, Langerhans cells, and anti-inflammatory cytokines such as IL-10^{14,59,76}. Whether SLE patients fail to control the inflammatory response to UVB in the skin and elsewhere is a critical question that will benefit from further understanding of the pathogenetic pathways involved.

Methods

Mice and UV irradiation. Male and female 12–16 week old C57BL/6 (B6, wild type), B6.cGAS $-/-$, or B6.*Ifnar* $-/-$ mice were shaved dorsally. Mice were anesthetized with isoflurane and a single dose of UVB light (500 mJ/cm²) was delivered either to the whole (Fig. 1) or half of the back (Figs. 2–5) using FS40T12/UVB bulbs (National Biological Corporation). The UVB light energy at the dorsal surface was measured with Photolight IL1400A radiometer with a SEL240/UVB detector (International Light Technologies). All animal experiments were approved by the Institutional Animal Care and Use Committee of the University of Washington, Seattle and guidelines for the care and use of animals during the research were followed. Mutant mice were kindly provided by Drs. Daniel Stetson and Michael Gale at the University of Washington.

Detection of Interferon Stimulated Gene (ISG) expression and IFN β production. Skin biopsies (6 mm) were performed prior to irradiation and at different time points after acute UVB injury: 6, 24, and 48 hours and tissue stored in RNA Later solution (Qiagen). Whole blood was collected prior to, 6 hr, and 24 hr following UVB light irradiation and red blood cells lysed. Kidneys were collected from mice following whole body cardiac perfusion with saline⁷⁷. RNA from skin and kidney was extracted by RNA Easy kit from Qiagen (Valencia, CA) and from blood cells using Quick RNA Miniprep (Zymogenetics). cDNA was synthesized using High Capacity cDNA synthesis kit (Applied Biosciences). ISG transcripts were selected according to previous studies of IFN response to UV and in *Trex* $-/-$ animals^{13,35} and quantified by real time quantitative PCR (qPCR) and normalized to *18S* (skin, kidney) or *Gapdh* (blood) transcript levels, using the primers described in Supplementary Table S1. The UV light dose used did not affect *18s* expression in the skin. Findings were confirmed using *gapdh* as the housekeeping gene, which was also not affected by skin UV exposure. Fold induction in ISG expression was determined using the standard formula $2^{(-\Delta\Delta Ct)}$ relative to baseline, i.e. skin prior to exposure to UVB. Mean IFN score was calculated as previously described²². The mean and standard deviation (SD) level of each ISG were determined in the skin or blood of mice prior to UV exposure ($mean_{preUV}$ and SD_{preUV}). These were then used to standardize the expression levels of each gene for each mouse at different times after exposure to UVB light (6 and 24 hr). The standardized expression levels were then summed for each mouse to derive an IFN expression score; i = expression of each ISG; $Gene\ i_{6\ or\ 24hr}$ = relative gene expression level 6 or 24 hours after exposure to UVB light; $Gene\ i_{preUV}$ = relative gene expression level in mice not exposed to UVB light; SD = standard deviation.

$$\sum_{i=1}^7 \frac{Gene\ i_{6\ or\ 24\ hr} - mean\ Gene\ i_{pre\ UV}}{SD\ (Gene\ i_{pre\ UV})}$$

Interferon beta (IFN β) protein levels in plasma were measured using Legendplex Mouse Inflammation Panel (Biolegend).

Flow cytometry analysis of inflammation. Skin biopsies (1 6 mm biopsy at 6 hr and 5 6 mm biopsies at 24 hr) from female B6 and cGAS $-/-$ mice were obtained prior to, 6 hr, and 24 hr after skin exposure to UVB light. Skin biopsies were processed as previously described¹³. Briefly, the tissue was minced finely and digested with

0.28 units/ml Liberase TM (Roche) and 0.1 mg/ml of Deoxyribonuclease I (Worthington) in PBS with Ca^{+2} and Mg^{+2} for 60 minutes at 37°C with shaking. Cells were passed through a 0.7 μm strainer, resuspended in RPMI and counted. Cells were treated with Fc Block TruStain FcX (Biolegend) and stained in PBS + 1% BSA. Surface staining was performed using mouse-specific fluorescent antibodies purchased from Biolegend: i) Myeloid panel: CD45 APC.Cy7, CD11b PerCP.Cy5.5, Ly6C Violet 610, Ly6G FITC and ii) T cell panel: CD45 APC.Cy7, CD8 PerCP.Cy5.5, CD4 Pe.Cy7, $\gamma\delta$ T PE. Samples were processed using CytoFLEX flow cytometer (Beckman Coulter) and data analyzed with FlowJo software v10 (Tree Star). Flow cytometry gating is demonstrated in Supplementary Figure S6. Immune cell populations and mean fluorescence intensities (MFI) of Sca-1 were determined using fluorescence minus one (FMO) controls. Numbers of different cell populations were determined based on total counted cell numbers and normalized to the area of a single biopsy (6 mm).

Immunofluorescence staining. Skin tissues were collected prior to and after (6 hr and 24 hr) mouse exposure to a single dose of UVB light and stored in optimal cutting temperature (OCT) medium. Frozen skin sections (6 μm) were fixed in cold acetone for 10 minutes and blocked (PBS/10% goat serum) for 30 minutes at room temperature. IFN β was detected using rabbit anti-mouse IFN β antibody (Novus Biologicals, 1:100) overnight at 4°C and secondary goat anti-rabbit Cy5 antibody (1:1000, Jackson ImmunoResearch) for 1 hr at RT. Non-specific staining was evaluated using rabbit IgG isotype control (at the same concentration as IFN β antibody) and secondary antibody as above. Tissues were mounted in DAPI containing Prolong Gold mounting medium (ThermoFischer). IF staining was imaged using Digital Fluorescence microscope EVOS FL.

In vivo treatment with hydroxychloroquine (HCQ) and ENPP1 inhibitor. Mice (B6) were treated with HCQ (25 mg/kg/day) for 3 weeks administered orally in Splenda-sweetened water. Controls were treated with Splenda-sweetened water alone. Following 3 weeks of treatment, mice were exposed to UVB light as described above. Blood and skin taken prior to and 6 hr after UV exposure were analyzed for ISG expression by qPCR and IFN scores derived, as described above. For treatment with ENPP1 inhibitor, mice were injected intradermally with 50 μl 100 μM STF1084 (two injections per mouse) (generously provided by Yinling Li at Stanford University), as used by Carozza *et al.* for intra-tumoral injections³⁰. After 30 minutes, mice were irradiated with a single dose of UVB light as described above. Skin biopsies were collected after 16 hr, a time point chosen to avoid toxicity³⁰, and processed for RNA isolation and QPCR as above. Skin was analyzed for ISG expression under four different conditions: vehicle alone, STF-1084 alone, vehicle + UVB, and STF1084 + UVB. Fold change in ISG expression was determined relative to vehicle alone control skin. Neither HCQ nor ENPP1 affected the expression of housekeeping genes used in qPCR studies (not shown). IFN scores were derived as described above.

Human phototesting and skin RNA Sequencing. Healthy volunteers were recruited from the University of Washington (UW, Seattle WA) and Philadelphia Veterans Affairs Medical Center (Pennsylvania, PA). All individuals signed an informed consent in respective IRB-approved protocols (University of Washington; HSD number 50655). All methods were carried out in accordance with relevant guidelines and regulations for human participants at the University of Washington. The sun-protected skin of 5 female healthy controls was exposed to two minimal erythematous doses (MED) of UVB light on the dorsal surface of the lower arm. Solar Simulator radiation was generated using a 150 W xenon arc, single port Berger Solar Simulator (Solar Light, Model # 16S-150/300, Glenside, PA). UG-5 and WG 320/1inch thick glass filters was fitted to give a wavelength spectrum that includes wavelengths above 290nm-400nm. A 6-mm punch skin biopsy was collected from unexposed skin, and from skin 6 hr and 24 hr after UV exposure. Tissue was stored in RNA later and samples from PA shipped to UW. Following RNA isolation at UW, the RNA yield was 2–3 μg RNA (all samples had RIN > 9.5). RNA sequencing was performed at Northwest Genomics Center at the University of Washington. cDNA libraries were prepared from 1 μg of total RNA using the TruSeq Stranded mRNA kit (Illumina, San Diego, CA) and the Sciclone NGSx Workstation (Perkin Elmer, Waltham, MA). Prior to cDNA library construction, ribosomal RNA was removed by means of poly-A enrichment. Each library was uniquely barcoded and subsequently amplified using a total of 13 cycles of PCR. Library concentrations were quantified using Qubit fluorometric quantitation (Life Technologies, Carlsbad, CA). Average fragment size and overall quality were evaluated with the DNA1000 assay on an Agilent 2100 Bioanalyzer. Each library was sequenced with paired-end 75 bp reads to a depth of 30 million reads on an Illumina HiSeq. 1500 sequencer.

RNAseq data processing and analysis. Raw RNAseq data (Fastq files) were demultiplexed and checked for quality (FastQC version 0.11.3). Next rRNA was digitally removed using Bowtie2 (version 2.2.5). Sufficient host reads (~thirty million) were then mapped to the Human genome (GRCh37) using STAR (2.4.2a) and then converted into gene counts with ht-seq (0.6.0). Both the genome sequence (fasta) and gene transfer files (gtf) were obtained using Illumina's igemomes website (https://support.illumina.com/sequencing/sequencing_software/igenome.html). Gene counts were then loaded in the R statistical programming language (version 3.2.1) and filtered by a row sum of fifty or more across all samples. Raw fastq files and count matrix were submitted to NCBI Gene Expression Omnibus (GEO) and available under accession GSE148535. Exploratory analysis and statistics were also run using R and bioconductor. The gene count matrix was normalized using EDGER and transformed to log counts per million (logCPM) using the voom through the limma bioconductor package (3.24.15). Statistical analysis (including differential expression) was performed using the limma package⁷⁸.

Interferon Z-score heatmap. Differential expression data was filtered for interferon genes and then plotted using the heatmap.2 function with the gplots bioconductor package in R⁷⁹.

IFN score analysis. IFN-I scores at 6 (n = 3) and 24 hr (n = 5) after UV were derived using the established IFN-I response gene dataset (188 of 212 genes were detected⁸). Relative expression of genes at baseline (prior to UV, n = 5) and at different times after UV was normalized as described above and IFN scores generated using the same formula as for mouse studies, using either all 188 genes or just the 7 genes used in mouse studies.

Statistical analysis. Data were analyzed using GraphPad Prism 7 software (GraphPad Software Inc.) and presented as mean + SEM. Statistical difference between two data groups was determined using Student's *t*-test. One way-ANOVA was used to determine statistical significance between three groups in human UV exposure studies. *P* < 0.05 was considered significant.

Data availability

The datasets generated in RNA Sequencing study are available on the NCBI GEO database under accession number GSE148535. The other data generated and/or analysed during this study are available from the corresponding author (SSG) upon reasonable request.

Received: 3 January 2020; Accepted: 21 April 2020;

Published online: 13 May 2020

References

- Schmidt, E., Tony, H. P., Brocker, E. B. & Kneitz, C. Sun-induced life-threatening lupus nephritis. *Annals of the New York Academy of Sciences* **1108**, 35–40, <https://doi.org/10.1196/annals.1422.004> (2007).
- Foering, K. *et al.* Characterization of clinical photosensitivity in cutaneous lupus erythematosus. *J Am Acad Dermatol* **69**, 205–213, <https://doi.org/10.1016/j.jaad.2013.03.015> (2013).
- Baechler, E. C. *et al.* Interferon-inducible gene expression signature in peripheral blood cells of patients with severe lupus. *Proceedings of the National Academy of Sciences of the United States of America* **100**, 2610–2615, <https://doi.org/10.1073/pnas.0337679100> (2003).
- Bennett, L. *et al.* Interferon and granulopoiesis signatures in systemic lupus erythematosus blood. *J Exp Med* **197**, 711–723, <https://doi.org/10.1084/jem.20021553> (2003).
- Crow, M. K., Kirou, K. A. & Wohlgemuth, J. Microarray analysis of interferon-regulated genes in SLE. *Autoimmunity* **36**, 481–490 (2003).
- Meller, S. *et al.* Ultraviolet radiation-induced injury, chemokines, and leukocyte recruitment: An amplification cycle triggering cutaneous lupus erythematosus. *Arthritis and rheumatism* **52**, 1504–1516, <https://doi.org/10.1002/art.21034> (2005).
- Der, E. *et al.* Single cell RNA sequencing to dissect the molecular heterogeneity in lupus nephritis. *JCI Insight* **2**, e93009, <https://doi.org/10.1172/jci.insight.93009> (2017).
- Der, E. *et al.* Tubular cell and keratinocyte single-cell transcriptomics applied to lupus nephritis reveal type I IFN and fibrosis relevant pathways. *Nat Immunol* **20**, 915–927, <https://doi.org/10.1038/s41590-019-0386-1> (2019).
- Bernard, J. J. *et al.* Ultraviolet radiation damages self noncoding RNA and is detected by TLR3. *Nature medicine* **18**, 1286–1290, <https://doi.org/10.1038/nm.2861> (2012).
- Gehrke, N. *et al.* Oxidative damage of DNA confers resistance to cytosolic nuclease TREX1 degradation and potentiates STING-dependent immune sensing. *Immunity* **39**, 482–495, <https://doi.org/10.1016/j.immuni.2013.08.004> (2013).
- Christou, E. A. A., Banos, A., Kosmara, D., Bertsias, G. K. & Boumpas, D. T. Sexual dimorphism in SLE: above and beyond sex hormones. *Lupus* **28**, 3–10, <https://doi.org/10.1177/0961203318815768> (2019).
- Liang, Y. *et al.* A gene network regulated by the transcription factor VGLL3 as a promoter of sex-biased autoimmune diseases. *Nat Immunol* **18**, 152–160, <https://doi.org/10.1038/ni.3643> (2017).
- Sontheimer, C., Liggitt, D. & Elkon, K. B. Ultraviolet B Irradiation Causes Stimulator of Interferon Genes-Dependent Production of Protective Type I Interferon in Mouse Skin by Recruited Inflammatory Monocytes. *Arthritis & rheumatology (Hoboken, N.J.)* **69**, 826–836, <https://doi.org/10.1002/art.39987> (2017).
- Wolf, S. J. *et al.* Ultraviolet light induces increased T cell activation in lupus-prone mice via type I IFN-dependent inhibition of T regulatory cells. *Journal of autoimmunity* **103**, 102291, <https://doi.org/10.1016/j.jaut.2019.06.002> (2019).
- Dunphy, G. *et al.* Non-canonical Activation of the DNA Sensing Adaptor STING by ATM and IFI16 Mediates NF- κ B Signaling after Nuclear DNA Damage. *Molecular cell* **71**, 745–760.e745, <https://doi.org/10.1016/j.molcel.2018.07.034> (2018).
- Zevini, A., Olagnier, D. & Hiscott, J. Crosstalk between Cytoplasmic RIG-I and STING Sensing Pathways. *Trends in immunology* **38**, 194–205, <https://doi.org/10.1016/j.it.2016.12.004> (2017).
- Sarkar, M. K. *et al.* Photosensitivity and type I IFN responses in cutaneous lupus are driven by epidermal-derived interferon kappa. *Annals of the rheumatic diseases* **77**, 1653–1664, <https://doi.org/10.1136/annrheumdis-2018-213197> (2018).
- Sharma, M. R., Werth, B. & Werth, V. P. Animal models of acute photodamage: comparisons of anatomic, cellular and molecular responses in C57BL/6J, SKH1 and Balb/c mice. *Photochemistry and photobiology* **87**, 690–698, <https://doi.org/10.1111/j.1751-1097.2011.00911.x> (2011).
- Patra, V., Wagner, K., Arulampalam, V. & Wolf, P. Skin Microbiome Modulates the Effect of Ultraviolet Radiation on Cellular Response and Immune Function. *iScience* **15**, 211–222, <https://doi.org/10.1016/j.isci.2019.04.026> (2019).
- Feng, X. *et al.* Association of increased interferon-inducible gene expression with disease activity and lupus nephritis in patients with systemic lupus erythematosus. *Arthritis and rheumatism* **54**, 2951–2962, <https://doi.org/10.1002/art.22044> (2006).
- Farkas, L., Beiske, K., Lund-Johansen, F., Brandtzaeg, P. & Jahnsen, F. L. Plasmacytoid dendritic cells (natural interferon- α / β -producing cells) accumulate in cutaneous lupus erythematosus lesions. *The American journal of pathology* **159**, 237–243 (2001).
- Braunstein, I., Klein, R., Okawa, J. & Werth, V. P. The interferon-regulated gene signature is elevated in subacute cutaneous lupus erythematosus and discoid lupus erythematosus and correlates with the cutaneous lupus area and severity index score. *Br J Dermatol* **166**, 971–975, <https://doi.org/10.1111/j.1365-2133.2012.10825.x> (2012).
- An, J., Woodward, J. J., Sasaki, T., Minie, M. & Elkon, K. B. Cutting edge: Antimalarial drugs inhibit IFN- β production through blockade of cyclic GMP-AMP synthase-DNA interaction. *Journal of immunology (Baltimore, Md.: 1950)* **194**, 4089–4093, <https://doi.org/10.4049/jimmunol.1402793> (2015).
- Chang, A. Y. *et al.* Response to antimalarial agents in cutaneous lupus erythematosus: a prospective analysis. *Archives of dermatology* **147**, 1261–1267, <https://doi.org/10.1001/archdermatol.2011.191> (2011).
- DeLong, J. H. *et al.* Cytokine- and TCR-Mediated Regulation of T Cell Expression of Ly6C and Sca-1. *The Journal of Immunology* **200**, 1761–1770, <https://doi.org/10.4049/jimmunol.1701154> (2018).
- Wu, J. *et al.* Cyclic GMP-AMP is an endogenous second messenger in innate immune signaling by cytosolic DNA. *Science* **339**, 826–830, <https://doi.org/10.1126/science.1229963> (2013).

27. Ashley, C. L., Abendroth, A., McSharry, B. P. & Slobedman, B. Interferon-Independent Upregulation of Interferon-Stimulated Genes during Human Cytomegalovirus Infection is Dependent on IRF3 Expression. *Viruses* **11**, 246, <https://doi.org/10.3390/v11030246> (2019).
28. Green, R., Ireton, R. C. & Gale, M. Jr. Interferon-stimulated genes: new platforms and computational approaches. *Mammalian genome: official journal of the International Mammalian Genome Society* **29**, 593–602, <https://doi.org/10.1007/s00335-018-9755-6> (2018).
29. Swanson, K. V. *et al.* A noncanonical function of cGAMP in inflammasome priming and activation. *The Journal of Experimental Medicine* **214**, 3611–3626, <https://doi.org/10.1084/jem.20171749> (2017).
30. Carozza, J. A. *et al.* Extracellular cGAMP is a cancer-cell-produced immunotransmitter involved in radiation-induced anticancer immunity. *Nature Cancer* **1**, 184–196, <https://doi.org/10.1038/s43018-020-0028-4> (2020).
31. Li, L. *et al.* Hydrolysis of 2'3'-cGAMP by ENPP1 and design of nonhydrolyzable analogs. *Nature chemical biology* **10**, 1043–1048, <https://doi.org/10.1038/nchembio.1661> (2014).
32. Bogoslawski, A., Butcher, E. C. & Kubes, P. Neutrophils recruited through high endothelial venules of the lymph nodes via PNAid intercept disseminating Staphylococcus aureus. *Proceedings of the National Academy of Sciences* **115**, 2449–2454, [10.1073/pnas.1715756115](https://doi.org/10.1073/pnas.1715756115) (2018).
33. Lanca, T. *et al.* Protective role of the inflammatory CCR2/CCL2 chemokine pathway through recruitment of type 1 cytotoxic gamma delta T lymphocytes to tumor beds. *Journal of immunology (Baltimore, Md.: 1950)* **190**, 6673–6680, doi:10.4049/jimmunol.1300434 (2013).
34. Penido, C. *et al.* Involvement of CC chemokines in $\gamma\delta$ T lymphocyte trafficking during allergic inflammation: the role of CCL2/CCR2 pathway. *International Immunology* **20**, 129–139, <https://doi.org/10.1093/intimm/dxm128> (2007).
35. An, J. *et al.* Inhibition of Cyclic GMP-AMP Synthase Using a Novel Antimalarial Drug Derivative in Trex1-Deficient Mice. *Arthritis & rheumatology (Hoboken, N.J.)* **70**, 1807–1819, <https://doi.org/10.1002/art.40559> (2018).
36. Psarras, A. *et al.* Plasmacytoid dendritic cells are functionally exhausted while non-haematopoietic sources of type I interferon dominate human autoimmunity. *bioRxiv*, 502047, <https://doi.org/10.1101/502047> (2018).
37. Rönnblom, L. Potential role of IFN α in adult lupus. *Arthritis Res Ther* **12**(Suppl 1), S3–S3, <https://doi.org/10.1186/ar2884> (2010).
38. Elkon, K. B. & Stone, V. V. Type I interferon and systemic lupus erythematosus. *Journal of interferon & cytokine research: the official journal of the International Society for Interferon and Cytokine Research* **31**, 803–812, <https://doi.org/10.1089/jir.2011.0045> (2011).
39. Blanco, P., Palucka, A. K., Gill, M., Pascual, V. & Banchereau, J. Induction of dendritic cell differentiation by IFN- α in systemic lupus erythematosus. *Science* **294**, 1540–1543, <https://doi.org/10.1126/science.1064890> (2001).
40. Connelly, K. L. *et al.* Longitudinal association of type I interferon-induced chemokines with disease activity in systemic lupus erythematosus. *Scientific Reports* **8**, 3268, <https://doi.org/10.1038/s41598-018-20203-9> (2018).
41. Crow, M. K., Olfieriev, M. & Kirou, K. A. Type I Interferons in Autoimmune Disease. *Annual Review of Pathology: Mechanisms of Disease* **14**, 369–393, <https://doi.org/10.1146/annurev-pathol-020117-043952> (2019).
42. Foerig, K. *et al.* Prevalence of self-report photosensitivity in cutaneous lupus erythematosus. *J Am Acad Dermatol* **66**, 220–228, <https://doi.org/10.1016/j.jaad.2010.12.006> (2012).
43. Furie, R. *et al.* Monoclonal antibody targeting BDCA2 ameliorates skin lesions in systemic lupus erythematosus. *The Journal of clinical investigation* **129**, 1359–1371, <https://doi.org/10.1172/jci.124466> (2019).
44. Lovgren, T., Eloranta, M. L., Bave, U., Alm, G. V. & Rönnblom, L. Induction of interferon-alpha production in plasmacytoid dendritic cells by immune complexes containing nucleic acid released by necrotic or late apoptotic cells and lupus IgG. *Arthritis and rheumatism* **50**, 1861–1872, <https://doi.org/10.1002/art.20254> (2004).
45. Bode, C. *et al.* Human plasmacytoid dendritic cells elicit a Type I Interferon response by sensing DNA via the cGAS-STING signaling pathway. *European journal of immunology* **46**, 1615–1621, <https://doi.org/10.1002/eji.201546113> (2016).
46. LaFleur, D. W. *et al.* Interferon-kappa, a novel type I interferon expressed in human keratinocytes. *The Journal of biological chemistry* **276**, 39765–39771, <https://doi.org/10.1074/jbc.M102502200> (2001).
47. Fujisawa, H., Kondo, S., Wang, B., Shivji, G. M. & Sauder, D. N. The expression and modulation of IFN-alpha and IFN-beta in human keratinocytes. *Journal of interferon & cytokine research: the official journal of the International Society for Interferon and Cytokine Research* **17**, 721–725, <https://doi.org/10.1089/jir.1997.17.721> (1997).
48. Catalina, M. D., Bachali, P., Geraci, N. S., Grammer, A. C. & Lipsky, P. E. Gene expression analysis delineates the potential roles of multiple interferons in systemic lupus erythematosus. *Commun Biol* **2**, 140–140, <https://doi.org/10.1038/s42003-019-0382-x> (2019).
49. Ni, G., Ma, Z. & Damania, B. cGAS and STING: At the intersection of DNA and RNA virus-sensing networks. *PLoS Pathog* **14**, e1007148–e1007148, <https://doi.org/10.1371/journal.ppat.1007148> (2018).
50. An, J. *et al.* Expression of Cyclic GMP-AMP Synthase in Patients With Systemic Lupus Erythematosus. *Arthritis & Rheumatology* **69**, 800–807, <https://doi.org/10.1002/art.40002> (2017).
51. Lood, C. *et al.* Neutrophil extracellular traps enriched in oxidized mitochondrial DNA are interferogenic and contribute to lupus-like disease. *Nature medicine* **22**, 146–153, <https://doi.org/10.1038/nm.4027> (2016).
52. Crow, Y. J. Type I interferonopathies: mendelian type I interferon up-regulation. *Current opinion in immunology* **32**, 7–12, <https://doi.org/10.1016/j.coi.2014.10.005> (2015).
53. Vanpouille-Box, C. *et al.* DNA exonuclease Trex1 regulates radiotherapy-induced tumour immunogenicity. *Nature communications* **8**, 15618–15618, <https://doi.org/10.1038/ncomms15618> (2017).
54. Li, T. & Chen, Z. J. The cGAS–cGAMP–STING pathway connects DNA damage to inflammation, senescence, and cancer. *The Journal of Experimental Medicine* **215**, 1287–1299, <https://doi.org/10.1084/jem.20180139> (2018).
55. Chiang, J. J. *et al.* Viral unmasking of cellular 5S rRNA pseudogene transcripts induces RIG-I-mediated immunity. *Nat Immunol* **19**, 53–62, <https://doi.org/10.1038/s41590-017-0005-y> (2018).
56. Li, Y. *et al.* LSm14A is a processing body-associated sensor of viral nucleic acids that initiates cellular antiviral response in the early phase of viral infection. *Proceedings of the National Academy of Sciences of the United States of America* **109**, 11770–11775, <https://doi.org/10.1073/pnas.1203405109> (2012).
57. Mustelin, T., Lood, C. & Giltiay, N. V. Sources of Pathogenic Nucleic Acids in Systemic Lupus Erythematosus. *Front Immunol* **10**, <https://doi.org/10.3389/fimmu.2019.01028> (2019).
58. Schuch, A. P., Moreno, N. C., Schuch, N. J., Menck, C. F. M. & Garcia, C. C. M. Sunlight damage to cellular DNA: Focus on oxidatively generated lesions. *Free Radical Biology and Medicine* **107**, 110–124, <https://doi.org/10.1016/j.freeradbiomed.2017.01.029> (2017).
59. Yamazaki, S. *et al.* Ultraviolet B-Induced Maturation of CD11b-Type Langerin(-) Dendritic Cells Controls the Expansion of Foxp3(+) Regulatory T Cells in the Skin. *Journal of immunology (Baltimore, Md.: 1950)* **200**, 119–129, <https://doi.org/10.4049/jimmunol.1701056> (2018).
60. Bashir, M. M., Sharma, M. R. & Werth, V. P. UVB and proinflammatory cytokines synergistically activate TNF-alpha production in keratinocytes through enhanced gene transcription. *J Invest Dermatol* **129**, 994–1001, <https://doi.org/10.1038/jid.2008.332> (2009).
61. Nickloff, J. A., Boss, M.-K., Allen, C. P. & LaRue, S. M. Translational research in radiation-induced DNA damage signaling and repair. *Transl Cancer Res* **6**, S875–S891, <https://doi.org/10.21037/tcr.2017.06.02> (2017).
62. Gaidt, M. M. *et al.* The DNA Inflammasome in Human Myeloid Cells Is Initiated by a STING-Cell Death Program Upstream of NLRP3. *Cell* **171**, 1110–1124.e1118, <https://doi.org/10.1016/j.cell.2017.09.039> (2017).

63. Li, A. *et al.* Activating cGAS-STING pathway for the optimal effect of cancer immunotherapy. *Journal of Hematology & Oncology* **12**, 35, <https://doi.org/10.1186/s13045-019-0721-x> (2019).
64. Vatner, R. E. & Janssen, E. M. STING, DCs and the link between innate and adaptive tumor immunity. *Molecular Immunology* **110**, 13–23, <https://doi.org/10.1016/j.molimm.2017.12.001> (2019).
65. Wang, H. *et al.* cGAS is essential for the antitumor effect of immune checkpoint blockade. *Proceedings of the National Academy of Sciences*, 201621363, <https://doi.org/10.1073/pnas.1621363114> (2017).
66. Harding, S. M. *et al.* Mitotic progression following DNA damage enables pattern recognition within micronuclei. *Nature* **548**, 466–470, <https://doi.org/10.1038/nature23470> (2017).
67. Ohkuri, T. *et al.* STING contributes to antiangioma immunity via triggering type I IFN signals in the tumor microenvironment. *Cancer Immunol Res* **2**, 1199–1208, <https://doi.org/10.1158/2326-6066.CIR-14-0099> (2014).
68. Christensen, J. E., de Lemos, C., Moos, T., Christensen, J. P. & Thomsen, A. R. CXCL10 is the key ligand for CXCR3 on CD8+ effector T cells involved in immune surveillance of the lymphocytic choriomeningitis virus-infected central nervous system. *Journal of Immunology (Baltimore, Md.: 1950)* **176**, 4235–4243, <https://doi.org/10.4049/jimmunol.176.7.4235> (2006).
69. Liu, J. *et al.* Local production of the chemokines CCL5 and CXCL10 attracts CD8+ T lymphocytes into esophageal squamous cell carcinoma. *Oncotarget* **6**, 24978–24989, <https://doi.org/10.18632/oncotarget.4617> (2015).
70. Scumpia, P. O. *et al.* Opposing roles of Toll-like receptor and cytosolic DNA-STING signaling pathways for *Staphylococcus aureus* cutaneous host defense. *PLoS Pathog* **13**, e1006496, <https://doi.org/10.1371/journal.ppat.1006496> (2017).
71. Maekawa, H. *et al.* Mitochondrial Damage Causes Inflammation via cGAS-STING Signaling in Acute Kidney Injury. *Cell Reports* **29**, 1261–1273, <https://doi.org/10.1016/j.celrep.2019.09.050> (2019).
72. MacLeod, A. S. *et al.* Skin-resident T cells sense ultraviolet radiation-induced injury and contribute to DNA repair. *Journal of Immunology (Baltimore, Md.: 1950)* **192**, 5695–5702, <https://doi.org/10.4049/jimmunol.1303297> (2014).
73. Volc-Platzer, B., Anegg, B., Milota, S., Pickl, W. & Fischer, G. Accumulation of gamma delta T cells in chronic cutaneous lupus erythematosus. *J Invest Dermatol* **100**, 84s–91s, <https://doi.org/10.1111/1523-1747.ep12356084> (1993).
74. Ghoreishi, M. & Dutz, J. P. A role for cutaneous gamma delta T cells in the development of systemic lupus erythematosus. *Arthritis Res Ther* **16**, A23, <https://doi.org/10.1186/ar4639> (2014).
75. Chang, J. J. *et al.* Higher expression of several interferon-stimulated genes in HIV-1-infected females after adjusting for the level of viral replication. *The Journal of infectious diseases* **208**, 830–838, <https://doi.org/10.1093/infdis/jit262> (2013).
76. Shipman, W. D. *et al.* A protective Langerhans cell-keratinocyte axis that is dysfunctional in photosensitivity. *Science translational medicine* **10**, <https://doi.org/10.1126/scitranslmed.aap9527> (2018).
77. Bethunaickan, R. & Davidson, A. Process and Analysis of Kidney Infiltrates by Flow Cytometry from Murine Lupus Nephritis. *Bio-protocol* **2**, e167, <https://doi.org/10.21769/BioProtoc.167> (2012).
78. Smyth, G. K. Linear models and empirical bayes methods for assessing differential expression in microarray experiments. *Statistical applications in genetics and molecular biology* **3**, Article3, <https://doi.org/10.2202/1544-6115.1027> (2004).
79. Gentleman, R. C. *et al.* Bioconductor: open software development for computational biology and bioinformatics. *Genome biology* **5**, R80, <https://doi.org/10.1186/gb-2004-5-10-r80> (2004).

Acknowledgements

This work was supported by National Institutes of Health R56 AR073848, R21 AR072377-01 and ACR Rheumatology Research Foundation Grant to KBE as well as NIH T32 AR007108 to SSG; Veterans Affairs Merit Review [I01BX000706] to VPW and NIH/NIAMS Werth R01AR071653. The RNA Sequencing work was supported by an NIH grant for the University of Washington Interdisciplinary Center for Exposures, Diseases, Genomics & Environment, P30ES07033. We thank Tomas Mustelin, Jeffrey Ledbetter, Edward Clark, and Erika Noss for insightful discussion. We thank Lingyin Li at Stanford University for generously providing the ENPPI inhibitor STF-1084. The authors declare no competing financial interests.

Author contributions

S.S.-G. and K.B.E. conceived the study and wrote the manuscript. S.S.-G., L.T., X.S., J.T., P.H., and R.B. conducted the experiments. S.S.-G. analyzed the data. J.A. and M.K. contributed to the conceptualization of the study and experimental design. M.G. and R.G. performed the analysis of RNA sequencing data. V.P.W., K.B.E., and A.K. conceptualized and executed human photo testing study. All authors critically reviewed and edited the manuscript.

Competing interests

The authors declare no competing interests.

Additional information

Supplementary information is available for this paper at <https://doi.org/10.1038/s41598-020-64865-w>.

Correspondence and requests for materials should be addressed to S.S.-G. or K.B.E.

Reprints and permissions information is available at www.nature.com/reprints.

Publisher's note Springer Nature remains neutral with regard to jurisdictional claims in published maps and institutional affiliations.



Open Access This article is licensed under a Creative Commons Attribution 4.0 International License, which permits use, sharing, adaptation, distribution and reproduction in any medium or format, as long as you give appropriate credit to the original author(s) and the source, provide a link to the Creative Commons license, and indicate if changes were made. The images or other third party material in this article are included in the article's Creative Commons license, unless indicated otherwise in a credit line to the material. If material is not included in the article's Creative Commons license and your intended use is not permitted by statutory regulation or exceeds the permitted use, you will need to obtain permission directly from the copyright holder. To view a copy of this license, visit <http://creativecommons.org/licenses/by/4.0/>.

© The Author(s) 2020